European Journal of Medicinal Chemistry 46 (2011) 150–159

Contents lists available at ScienceDirect

European Journal of Medicinal Chemistry

journal homepage: http://www.elsevier.com/locate/ejmech

Original article

# Co(III), Ni(II), Zn(II) and Cd(II) complexes with 2-acetyl-2-thiazoline thiosemicarbazone: Synthesis, characterization, X-ray structures and antibacterial activity

E. Viñuelas-Zahínos [a], F. Luna-Giles [a,*], P. Torres-García [a], M.C. Fernández-Calderón [b,c]

[a] Departamento de Química Orgánica e Inorgánica, Facultad de Ciencias, Universidad de Extremadura, 06071 Badajoz, Spain
[b] Departamento de Ciencias Biomédicas, Área de Microbiología, Facultad de Medicina, Universidad de Extremadura, 06071 Badajoz, Spain
[c] Centro de Investigación Biomédica en Red en Bioingeniería, Biomateriales y Nanomedicina CIBER-BBN Badajoz, Spain

ARTICLE INFO

*Article history:*
Received 28 May 2010
Received in revised form
20 October 2010
Accepted 29 October 2010
Available online 4 November 2010

*Keywords:*
Thiosemicarbazone
Thiazoline
Crystal structure
Metal complexes
Antibacterial activity

ABSTRACT

The new ligand 2-acetyl-2-thiazoline thiosemicarbazone (HATtsc) and the complexes $[Co(ATtsc)_2]_2[CoCl_4]\cdot 2H_2O$ (**1**), $[Co(ATtsc)_2]NO_3\cdot H_2O$ (**2**), $[Ni(HATtsc)_2](NO_3)_2$ (**3**), $[ZnCl_2(HATtsc)]\cdot CH_3CN$ (**4**), $[\{CdCl(HATtsc)\}_2(\mu\text{-}Cl)_2]\cdot 2H_2O$ (**5**) and $[\{Cd(NO_3)(HATtsc)\}_2(\mu\text{-}NO_3)_2]$ (**6**) were isolated and characterized by a variety of physico-chemical techniques and X-ray diffraction. The structure of HATtsc in **1** and **2** presented a thiolate form while in **3**–**6** the thione form was present, as it was in free ligand. In addition, we studied the antibacterial activity of the ligand and complexes **2**–**6** against some representative bacteria. Cd(II) complexes were more active against *Staphylococcus epidermidis*, *Staphylococcus aureus*, *Enterococcus faecalis*, *Escherichia coli* and *Bacillus subtilis* than organic ligand. Conversely, Cd(II) compounds seemed to interfere in the cell separation of *B. subtilis*.



## 1. Introduction

Thiazolines are five-membered heterocycles present in a great number of natural and synthetic products, many of which present antibiotic activity, such as micacocidin [1] and bacitracin A [2]. Metallic ions have been shown to play an important role in the biological activity of thiazoline derivative compounds, in such a way that, in some cases, activity is enhanced or only takes place in the presence of these ions. An example of this is bacitracin A, whose activity is highly enhanced by Zn(II) ion [2]. On the other hand, thiosemicarbazones are a type of N,S-donor ligands that have been extensively used in coordination chemistry because of their versatility, since they exist as thione-thiol tautomers, and can bind to a metal centre in the neutral or the anionic forms, acting as monodentate, bidentate or bridge ligands [3]. Additionally, thiosemicarbazone derivatives have recently aroused considerable interest in chemistry and biology because of the antiviral, antibacterial and antitumoral activity of many of them [4–7]. In some cases biological activity associated to a metal complex is greater than the corresponding free thiosemicarbazone ligand, as in, for example, some Cd(II) complexes of (3-thiophene) aldehyde thiosemicarbazone against several bacteria and fungi [8], Ni(II) and Cu(II) complexes of the ligand (2-pyridinecarboxaldehyde) thiosemicarbazone against Gram-positive and Gram-negative bacteria [9], or several Zn(II) complexes of (2-acetylpyridine) thiosemicarbazone against selected bacteria [10].

In the present paper we report the structural and antibacterial activity of the thiazoline/thiosemicarbazone derivative 2-acetyl-2-thiazoline thiosemicarbazone (HATtsc), and its cobalt(III), nickel(II), zinc(II) and cadmium(II) complexes. Results are reported on the isolation and characterization by X-ray single-crystal diffractometry, elemental analysis, NMR, IR and UV–Vis spectra of HATtsc, and a study is made of the solid phases obtained by reaction of HATtsc with the corresponding inorganic salts through elemental analysis, NMR, IR, electronic spectroscopy and X-ray single-crystal diffractometry. In addition, antibacterial activity against *Staphylococcus epidermidis*, *Staphylococcus aureus*, *Enterococcus faecalis*, *Bacillus subtilis*, *Escherichia coli* and *Pseudomonas aeruginosa* is described.

## 2. Chemistry

The precursor 2-acetyl-2-thiazoline was synthesized according to the method described by Doornbos and Peer [11]. The ligand 2-acetyl-2-thiazoline thiosemicarbazone (HATtsc) was obtained by means of reaction of 2-acetyl-2-thiazoline with thiosemicarbazide in acetonitrile and glacial acetic acid.

* Corresponding author. Tel.: +34 924 289 397; fax: +34 924 271 149.
*E-mail address:* pacoluna@unex.es (F. Luna-Giles).

0223-5234/$ – see front matter © 2010 Elsevier Masson SAS. All rights reserved.
doi:10.1016/j.ejmech.2010.10.030

Metal complexes were prepared by reacting a solution of the metal(II) salt (chloride or nitrate) in ethanol:acetonitrile (2:1) with a solution of HATtsc in the same solvent, in a 1:1 or 1:2, M:L molar ratio. The structures of the metal complexes were confirmed by elemental analysis, IR spectroscopy and X-ray diffraction. In Co(III) and Ni(II) complexes, UV–Vis–NIR diffuse reflectance was used for characterization. A general scheme which represents the strategy employed for the synthesis of the ligand and metal complexes is illustrated in Scheme 1.

## 3. Pharmacology

The newly synthesized compounds were screened for their *in vitro* antibacterial activity against the following organisms which were obtained directly from ATCC collections: *Staphylococcus epidermidis* ATCC 12228, *Staphylococcus aureus* ATCC 29213, *Enterococcus faecalis* ATCC 29212, *Bacillus subtilis* ATCC 12432, *Escherichia coli* ATCC 25922 and *Pseudomonas aeruginosa* ATCC 27853 using the serial dilutions broth method for the determination of MIC.

## 4. Results and discussion

### 4.1. Description of the structures

The molecular structures of ligand and complexes (or complex cations) together with the atomic numbering scheme are shown in Figs. 1–6. Selected bond lengths and angles are listed in Tables 1 and 2.

In the crystal structure of ligand HATtsc only the *E* isomer in the imine bond is observed. It is known that the thiosemicarbazone group can present a thione-thiol tautomerism. The C(6)–S(2) distance is similar to that found in other thiosemicarbazones which present the thione form in the solid state [12–14], which indicates that HATtsc is in that form.

The unit cell of **1** contains eight $[Co(ATtsc)_2]^+$ complex cations, four $[CoCl_4]^{2-}$ complex anions and eight crystallization water molecules. Thus, the compound can be formulated as $[Co(ATtsc)_2]_2[CoCl_4]\cdot 2H_2O$. The coordination geometry around Co(III) ion in this cation can be described as a distorted octahedron, the cobalt atom being bonded to two tridentate ATtsc molecules in such a way that four fused-in-pairs chelate rings are formed (Fig. 2). The C–S bond distance increased from

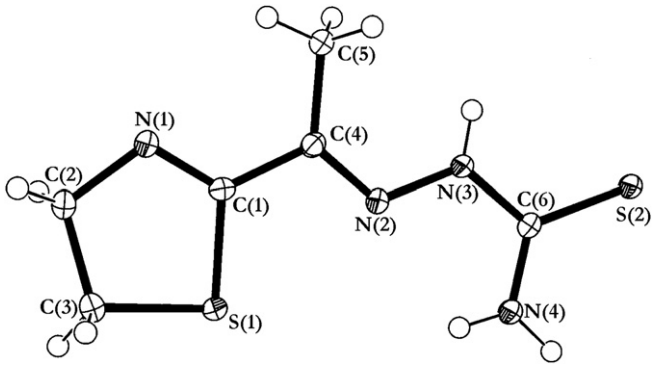


**Fig. 1.** Crystal structure of HATtsc, showing the atom-numbering scheme. The thermal ellipsoids are plotted at the 50% probability level.

1.688(1) Å in the free ligand HATtsc to 1.738(3) Å [S(2)–C(6)] and 1.743 (2) Å [S(4)–C(12)] in the cobalt complex. Likewise, there was a reduction of the carbon-hydrazinic nitrogen bond length from 1.365(3) Å [N(3)–C (6)] in the free ligand to 1.339(3) Å [N(3)–C(6)] and 1.325(3) Å [N(7)–C (12)] in the complex. These facts indicate that the ligand is deprotonated and shifts from the thione to the thiolate form, in such a way that the negative charge is delocalized between the two bonds [5].

With regard to complex **2**, the complex salt can be formulated as $[Co(ATtsc)_2]NO_3\cdot H_2O$, the complex cation being the same as in **1** as described above.

Complex **3** can be formulated as the complex salt $[Ni(HATtsc)_2](NO_3)_2$. The monoclinic unit cell contains four complex cations $[Ni(HATtsc)_2]^{2+}$ and eight nitrate anions. As can be observed in Fig. 3, the nickel atom is coordinated to two organic HATtsc molecules that behave as $N_2S$ tridentate ligands (Fig. 3). Thus, the coordination polyhedron around the Ni(II) ion can be described as a distorted octahedron.

In the complex molecule of **4** the Zn(II) ion is five-coordinated by two chlorine ligands and two nitrogen and one sulfur atom from an HATtsc ligand (Fig. 4). The coordination geometry around the zinc atom can be described as intermediate between square pyramid and trigonal bipyramid, closer to the latter ($\tau = 0.58$ [15] and $\Delta = 0.32$ [16]). The equatorial plane in the bipyramid is

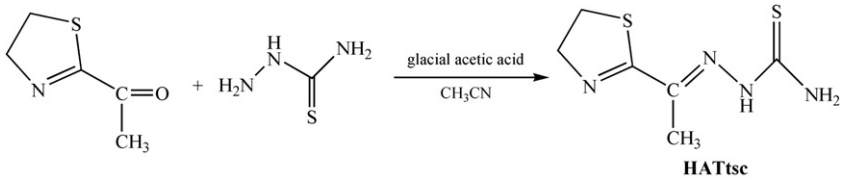


$$2\,HATtsc + CoCl_2\cdot 6H_2O \xrightarrow{EtOH:CH_3CN\ (2:1)} [Co(ATtsc)_2]_2[CoCl_4]\cdot 2H_2O\ (\mathbf{1})$$

$$2\,HATtsc + Co(NO_3)_2\cdot 6H_2O \xrightarrow{EtOH:CH_3CN\ (2:1)} [Co(ATtsc)_2]NO_3\cdot H_2O\ (\mathbf{2})$$

$$2\,HATtsc + Ni(NO_3)_2\cdot 6H_2O \xrightarrow{EtOH:CH_3CN\ (2:1)} [Ni(HATtsc)_2](NO_3)_2\ (\mathbf{3})$$

$$HATtsc + ZnCl_2 \xrightarrow{EtOH:CH_3CN\ (2:1)} [ZnCl_2(HATtsc)]\cdot CH_3CN\ (\mathbf{4})$$

$$HATtsc + CdCl_2\cdot 2{,}5H_2O \xrightarrow{EtOH:CH_3CN\ (2:1)} [\{CdCl(HATtsc)\}_2(\mu\text{-}Cl)_2]\cdot 2H_2O\ (\mathbf{5})$$

$$HATtsc + Cd(NO_3)_2\cdot 4H_2O \xrightarrow{EtOH:CH_3CN\ (2:1)} [\{Cd(NO_3)(HATtsc)\}_2(\mu\text{-}NO_3)_2]\ (\mathbf{6})$$

**Scheme 1.** Preparation of ligand and metal complexes.

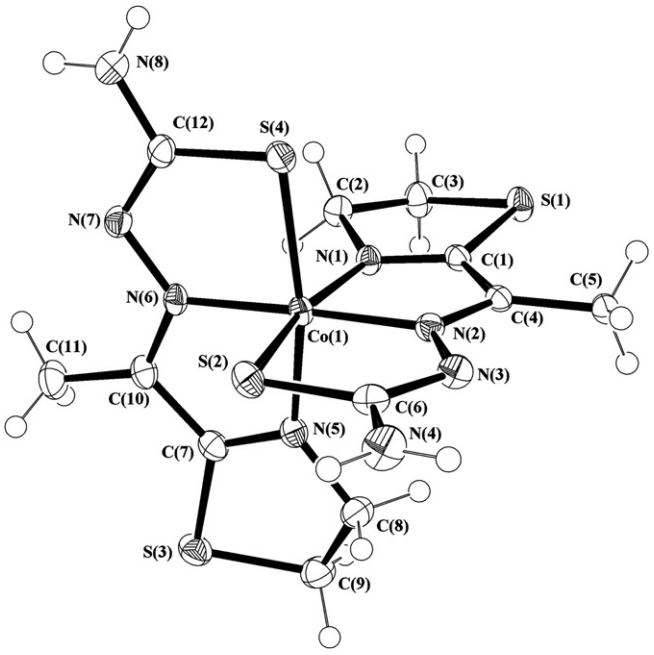


**Fig. 2.** Crystal structure of complex cation $[Co(ATtsc)_2]^+$ in **1**. The thermal ellipsoids are plotted at the 50% probability level.

constituted by atoms Cl(1), Cl(2) and N(2), whereas the axial positions are occupied by nitrogen N(1) and sulfur S(2).

The X-ray study of **5** revealed that the crystal is constituted by centrosymmetric dimeric molecules $[\{CdCl(HATtsc)\}_2(\mu\text{-}Cl)_2]$ and two crystallization water molecules per dimmer (Fig. 5). In dimeric molecules there are two six-coordinated Cd(II) centres, each of which is linked to a $N_2S$ tridentate HATtsc ligand. The remaining coordination sites are occupied by three chlorine atoms, two of which are bridging ligands. The bridging unit $Cd_2Cl_2$ is strictly planar due to the presence of the crystallographic inversion centre in the middle of the dimer. The environment around each cadmium atom may be described as a highly distorted octahedral geometry.

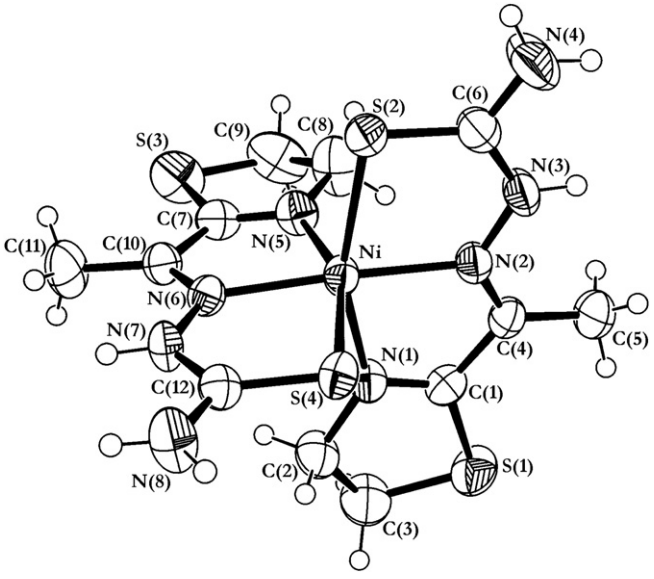


**Fig. 3.** Crystal structure of complex cation $[Ni(HATtsc)_2]^{2+}$ in **3**. The thermal ellipsoids are plotted at the 50% probability level.

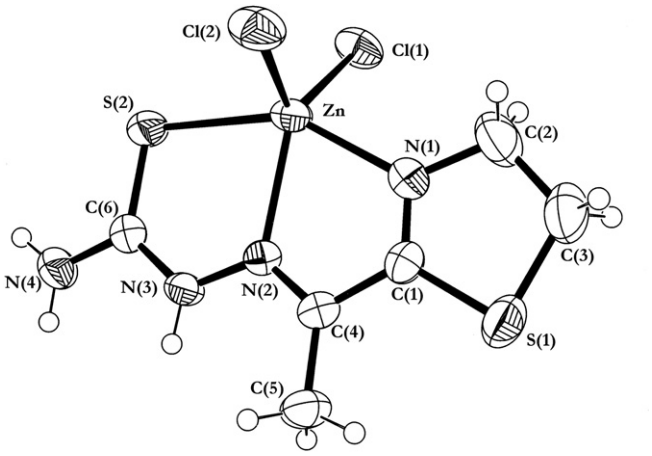


**Fig. 4.** Crystal structure of $[ZnCl_2(HATtsc)]$ in **4**. The thermal ellipsoids are plotted at the 50% probability level.

The crystal of **6** is made up of dimeric molecules $[\{Cd(NO_3)(HATtsc)\}_2(\mu\text{-}NO_3)_2]$ in which the cadmium atoms are bridged by two nitrate ligands. This structure is very similar to that found in **5**, already described, with the main difference that chlorine bridging ligands are substituted by monodentate bridging nitrate ligands, as is shown in Fig. 6.

It should be pointed out that in complexes **3**–**6**, in contrast to **1** and **2**, the organic ligand presents a thione form, in a similar way to free state, as can be deduced from the similarity of S(2)–C(6) and N(3)–C(6) bond distances both in the complexes and in the free ligand. Another difference in all the complexes with respect to the structure of the free ligand HATtsc is the degree of rotation around the C(1)–C(4) [also C(7)–C(10) in **1**–**3**] and C(6)–N(3) [also C(12)–N(7) in **1**–**3**] bonds, which permits coordination through N(1) and S(2) [or N(5) and S(4) in **1**–**3**].

Since the thiosemicarbazone moiety has both hydrogen bond donors and hydrogen bond acceptors, the species provide the possibility of forming hydrogen bonds in the crystal. Thus, an intermolecular hydrogen bond network stabilises the crystal structure of HATtsc. In this network the thione sulfur atoms and thiazoline nitrogen atoms act as hydrogen acceptors, while amino nitrogen atoms N(3) and N(4) act as donors. Table 3 contains the geometric parameters and Fig. 7 shows a representation of the bond network.

Similarly, the crystal structures of the complexes are stabilized by intermolecular hydrogen bonds (see Figs in Supplementary data), and differ in the hydrogen bond donors and acceptors (see Table 3).

### 4.2. IR spectra

The tentative assignments of the significant IR spectral bands of HATtsc and its metal complexes are presented in Table 4. With respect to the possible thione-thiol tautomerism in the ligand, the absence of the $\nu$(S–H) vibration band at 2750 $cm^{-1}$ as well as the presence of bands due to the $\nu$(C=S) vibration at 846 $cm^{-1}$ and to the $\nu$(N–H) vibration between 3191 and 3064 $cm^{-1}$ confirm that in the solid state the thione tautomer is present [17]. It can be observed that in all complexes the band that involved thiazoline $\nu$(C=N) endocyclic vibration and $\nu$(C=N) exocyclic vibration in the ligand is split after coordination in two bands which suffer a negative and a positive shift, respectively. This feature is indicative for coordination through the imine and thiazoline nitrogen atoms [18–20]. Furthermore, the presence of a second band assigned to a $\nu$(C=N) vibration mode in **1** and **2** is in good

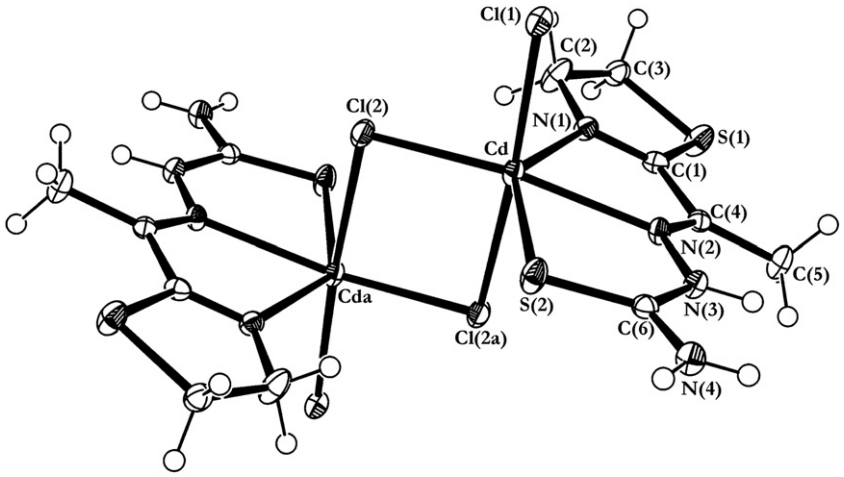


**Fig. 5.** Crystal structure of $[\{CdCl(HATtsc)\}_2(\mu\text{-}Cl)_2]$ in **5**. The thermal ellipsoids are plotted at the 50% probability level.

agreement with the ATtsc ligand in its thiolate form. On the other hand, the thioamide IV vibration band $\nu$(C=S) suffers a negative shift in all complexes with respect to the free ligand, thus indicating that the exocyclic sulfur atom is involved in coordination to the metal ion [20,21].

### 4.3. Electronic spectra

The reflectance spectrum for complex **1** present the multiple absorptions corresponding to $[CoCl_4]^{2-}$at 5260 $cm^{-1}$ ($\nu_2[^4T_{1g}(F) \leftarrow {}^4A_2(F)]$) and at 14600 $cm^{-1}$ ($\nu_3[^4T_1(P) \leftarrow {}^4A_2(F)]$) [22]. Additionally, the spectra of **1** and **2** show one intense band at 20570 $cm^{-1}$ for **1** and at 22520 for **2**, each one presenting several shoulders, corresponding to the octahedral Co(III) complex cation. The electronic spectra of spin paired trivalent cobalt(III) complexes of approximate $O_h$ symmetry have the following assignments of d–d bands: $\nu_1[^1T_{1g}(I) \leftarrow {}^1A_{1g}(I)]$, $\nu_2[^1T_{2g}(I) \leftarrow {}^1A_{1g}(I)]$, $\nu_3[^3T_{1g}(H) \leftarrow {}^1A_{1g}(I)]$, $\nu_4[^3T_{2g}(H) \leftarrow {}^1A_{1g}(I)]$ [23]. According to the data on other similar complexes found in the literature [22–25], the shoulders may be assigned as follows: 12990 $cm^{-1}$ ($\nu_3[^3T_{1g}(H) \leftarrow {}^1A_{1g}(I)]$), 26315 $cm^{-1}$ ($\nu_2[^1T_{2g}(I) \leftarrow {}^1A_{1g}(I)]$), 20580 $cm^{-1}$ ($\nu_1[^1T_{1g}(I) \leftarrow {}^1A_{1g}(I)]$) for **1** and 16550 $cm^{-1}$ ($\nu_4[^3T_{2g}(H) \leftarrow {}^1A_{1g}(I)]$), 13330 $cm^{-1}$ ($\nu_3[^3T_{1g}(H) \leftarrow {}^1A_{1g}(I)]$), 26880 $cm^{-1}$ ($\nu_2[^1T_{2g}(I) \leftarrow {}^1A_{1g}(I)]$) and 22520 $cm^{-1}$ ($\nu_1[^1T_{1g}(I) \leftarrow {}^1A_{1g}(I)]$) for **2**. The shoulders that appear at 23150 and 32258 $cm^{-1}$ in **1** and 26800 $cm^{-1}$ and 31060 $cm^{-1}$ for **2** have been assigned to a Co(III) → S charge transfer band and an organic ligand $\pi \rightarrow \pi^*$ transition, respectively. However, when **1** is dissolved in water, its spectrum is different from that observed in solid state presenting one intense band with two shoulders registered between 200 nm and 500 nm. Likewise, the spectrum does not present any of the characteristic multiple absorptions of tetrachlorocobaltate(II) [22], which indicates that the integrity of **1** does not remain in solution. For this reason **1** was rejected for antibacterial studies.

The electronic spectrum of complex **3** shows two massive absorption zones. The first consists of a band with a shoulder at 18050 $cm^{-1}$, a maximum at 27470 $cm^{-1}$ and another shoulder at 35970 $cm^{-1}$. These last two signals may be assigned to a charge transfer band and to a $\pi \rightarrow \pi^*$ transition from HATtsc, respectively, while the first shoulder is assigned to the $\nu_2[^3T_{1g}(F) \leftarrow {}^3A_{2g}(F)]$ d–d transition. The second zone consists of a broad band with several maximums between 12500 and 10000 $cm^{-1}$. The weighted mean of

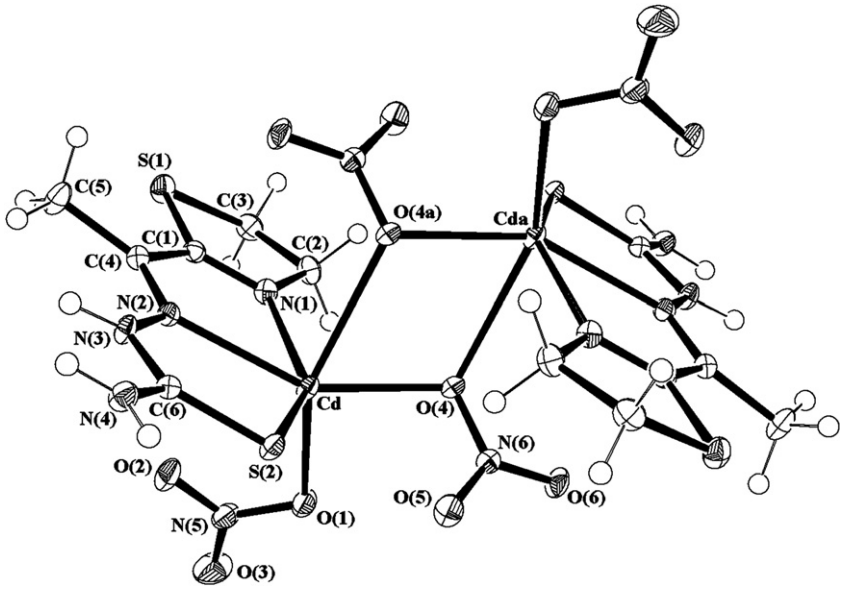


**Fig. 6.** Crystal structure of **6**. The thermal ellipsoids are plotted at the 50% probability level.

**Table 1**
Selected bond lengths (Å) and angles (°) for HATtsc, **1**, **2** and **3**.

| HATtsc | | **1** | | **2** | | **3** | |
|---|---|---|---|---|---|---|---|
| S(1)–C(1) | 1.773(1) | Co(1)–N(1) | 1.933(2) | Co–N(1) | 1.936(3) | Ni–N(1) | 2.050(3) |
| N(2)–C(4) | 1.290(2) | Co(1)–N(2) | 1.903(2) | Co–N(2) | 1.897(3) | Ni–N(2) | 2.041(3) |
| N(3)–C(6) | 1.364(2) | Co(1)–N(5) | 1.939(2) | Co–N(5) | 1.930(3) | Ni–N(5) | 2.072(3) |
| C(1)–N(1) | 1.276(2) | Co(1)–N(6) | 1.900(2) | Co–N(6) | 1.903(3) | Ni–N(6) | 2.038(3) |
| N(2)–N(3) | 1.368(1) | Co(1)–S(2) | 2.225(1) | Co–S(2) | 2.216(1) | Ni–S(2) | 2.400(2) |
| S(2)–C(6) | 1.688(1) | Co(1)–S(4) | 2.234(1) | Co–S(4) | 2.229(1) | Ni–S(4) | 2.403(2) |
| N(1)–C(1)–S(1) | 118.1(1) | N(1)–Co(1)–S(2) | 167.8(1) | N(1)–Co–S(2) | 167.0(1) | N(1)–Ni–S(2) | 159.2(1) |
| N(2)–N(3)–C(6) | 118.0(1) | N(1)–Co(1)–S(4) | 88.2(1) | N(1)–Co–S(4) | 91.4(1) | N(1)–Ni–S(4) | 90.2(1) |
| N(3)–C(6)–S(2) | 119.9(1) | N(2)–Co(1)–S(2) | 85.4(1) | N(2)–Co–S(2) | 85.2(1) | N(2)–Ni–S(2) | 81.9(1) |
| N(1)–C(1)–C(4) | 123.2(1) | N(2)–Co(1)–S(4) | 95.7(1) | N(2)–Co–S(4) | 95.6(1) | N(2)–Ni–S(4) | 101.9(1) |
| N(2)–C(4)–C(1) | 113.6(1) | N(5)–Co(1)–S(2) | 90.6(1) | N(5)–Co–S(2) | 89.2(1) | N(5)–Ni–S(2) | 93.8(1) |
| | | N(5)–Co(1)–S(4) | 167.4(1) | N(5)–Co–S(4) | 167.1(1) | N(5)–Ni–S(4) | 158.6(1) |
| | | N(6)–Co(1)–S(2) | 92.5(1) | N(6)–Co–S(2) | 94.8(1) | N(6)–Ni–S(2) | 104.2(1) |
| | | N(6)–Co(1)–S(4) | 85.6(1) | N(6)–Co–S(4) | 85.1(1) | N(6)–Ni–S(4) | 81.6(1) |

all these maximums (11340 $cm^{-1}$) has been assigned to $\nu_1[^3T_{2g}(F) \leftarrow {}^3A_{2g}(F)]$ transition. This spectral pattern is typical of octahedral nickel(II) complexes [26,27]. It can be observed that the diffuse reflectance spectrum of **3** is similar to its absorption spectrum in water solution, thus proving that the coordination environment remains unaltered in solution.

### 4.4. NMR spectra

The NMR spectral data of the ligand and its complexes were recorded in DMSO-$d_6$. In the case of **4**, **5** and **6**, they are very poorly soluble in DMSO and so only their $^1$H NMR spectra were recorded. Spectra of complexes are slightly modified with respect to the free ligand, and show the same multiplicity of the signals and slight changes in the chemical shifts. These $^1$H NMR spectra are in agreement with the thione tautomer on the basis of precedent data and support the structural integrity of these complexes in solution.

Conversely, the diamagnetic Co(III) complex **2** is soluble in DMSO, thus when the $^1$H NMR data are compared with those of the free ligand, several differences can be observed: (i) the peak corresponding to the proton attached to N(3) is missing, which is evidence of the deprotonation of the ligand; (ii) the signals at 7.29 and 8.64 ppm assigned to the $NH_2$ group in HATtsc merge as one signal at 8.38 ppm in the complex since these protons are no longer diasterotopic upon coordination because of the reduction of C(1)–N(1) bond order; (iii) the upper field shift observed for C(2) protons can be interpreted as a sign of the participation in coordination of the thiazoline nitrogen atom. Likewise, with respect to the $^{13}$C NMR spectrum, the C(2) signal at 65.3 ppm in the ligand is shifted upfield in the complex spectrum indicating the participation of N(1) in the coordination. The C(1) and C(6) signals suffer changes that could be due to the coordination through N(1) and S(2).

In order to investigate the stability of complex **2** in water solution, the NMR study in $D_2O$ was carried out, with results very similar to those obtained for DMSO-$d_6$, thus indicating that the octahedral geometry is maintained in both solutions.

**Table 2**
Selected bond lengths (Å) and angles (°) for **4**, **5** and **6**.

| **4** | | **5** | | **6** | |
|---|---|---|---|---|---|
| Zn–Cl(1) | 2.284(1) | Cd–N(1) | 2.331(3) | Cd–N(1) | 2.291(2) |
| Zn–N(1) | 2.140(2) | Cd–N(2) | 2.419(3) | Cd–N(2) | 2.400(2) |
| Zn–S(2) | 2.491(1) | Cd–S(2) | 2.608(1) | Cd–S(2) | 2.527(1) |
| Zn–Cl(2) | 2.267(1) | Cd–Cl(1) | 2.603(1) | Cd–O(1) | 2.342(2) |
| Zn–N(2) | 2.214(2) | Cd–Cl(2) | 2.533(1) | Cd–O(4) | 2.320(1) |
| | | Cd–Cl(2a) | 2.816(1) | Cd–O(4a) | 2.667(2) |
| Cl(1)–Zn–S(2) | 100.1(1) | N(1)–Cd–S(2) | 140.7(1) | N(1)–Cd–S(2) | 143.8(1) |
| Cl(2)–Zn–S(2) | 100.2(1) | Cl(1)–Cd–S(2) | 95.3(1) | O(1)–Cd–S(2) | 109.7(1) |
| S(2)–Zn–N(2) | 76.8(1) | N(2)–Cd–S(2) | 73.0(1) | N(2)–Cd–S(2) | 75.0(1) |
| S(2)–Zn–N(1) | 149.1(1) | Cl(2)–Cd–S(2) | 117.2(3) | O(4)–Cd–S(2) | 117.4(1) |
| | | S(2)–Cd–Cl(2a) | 90.9(3) | S(2)–Cd–O(4a) | 95.8(1) |

### 4.5. Antibacterial activity

The HATtsc ligand and its metal complexes were screened for antibacterial activity against Gram-positive (*E. faecalis*, *B. subtilis*, *S. aureus*, *S. epidermidis*) and Gram-negative bacteria (*E. coli*, *P. aeruginosa*) (see Table 5). To compare antibacterial activities shown by the synthesized compounds, data from the standard drug ampicilin, belonging to the penicillin family, against the same bacterial strains published by Clinical and Laboratory Standards Institute [28] and other authors in Ref. [29] were used.

**Table 3**
Hydrogen bond parameters for HATtsc, **1**, **2**, **3**, **4**, **5** and **6**.

| D–H···A | Position of A | A···D (Å) | A···H–D (°) |
|---|---|---|---|
| HATtsc | | | |
| N(4)–H(4A)···N(1) | x, y − 1, z | 3.011(2) | 162(2) |
| N(3)–H(3C)···S(2) | −x − 0.5, −y + 0.5, −z | 3.444(1) | 174(2) |
| **1** | | | |
| N(4)–H(4A)···O(1W) | x, y, z | 2.824(5) | 148.4 |
| N(4)–H(4B)···Cl(2) | −x + 0.5, −y + 1.5, −z + 1 | 3.236(2) | 138.7 |
| N(8)–H(8B)···O(1W) | −x + 0.5, y + 0.5, −z + 0.5 | 2.878(5) | 133.0 |
| **2** | | | |
| N(8)–H(8D)···O(1W) | x, y, z | 2.842(9) | 169(4) |
| N(4)–H(4A)···N(3) | −x + 1, y, z + 1.5 | 3.049(4) | 153(1) |
| **3** | | | |
| N(4)–H(4B)···O(5) | x, y, z | 3.086(2) | 156.2 |
| N(8)–H(8C)···O(3) | −x + 1, −y, −z | 3.797(3) | 169.5 |
| N(7)–H(7)···O(1) | −x + 1, −y, −z | 2.766(3) | 155.0 |
| N(4)–H(4A)···O(6) | −x, y − 0.5, −z + 0.5 | 3.017(2) | 141.8 |
| N(3)–H(3)···O(4) | −x, y − 0.5, −z + 0.5 | 2.845(2) | 166.1 |
| N(8)–H(8D)···O(6) | x, −y + 1.5, z − 0.5 | 2.924(2) | 169.4 |
| **4** | | | |
| N(3)–H(3)···Cl(1) | −x, −y + 1, −z + 2 | 3.287(2) | 131.3 |
| N(4)–H(4A)···Cl(2) | −x + 1, −y + 1, −z + 2 | 3.232(3) | 141.4 |
| N(4)–H(4B)···N(5) | −x + 1, −y + 1, −z + 2 | 2.977(3) | 161.9 |
| **5** | | | |
| N(4)–H(4B)···O(1W) | x − 1, y, z | 2.897(5) | 166(4) |
| N(3)–H(3C)···Cl(1) | −x, −y + 1, −z + 1 | 3.131(3) | 154(3) |
| N(4)–H(4A)···Cl(1) | −x, −y + 1, −z + 1 | 3.361(4) | 148(3) |
| O(1W)–H(1W)···Cl(2) | x, y, z + 1 | 3.271(3) | 166(2) |
| O(1W)–H(2W)···Cl(1) | −x + 1, −y, −z + 1 | 3.343(3) | 169(1) |
| **6** | | | |
| N(3)–H(3)···O(1) | −x + 0.5, y − 0.5, −z + 1.5 | 2.898(1) | 160.0 |
| N(4)–H(4B)···O(5) | −x + 1, −y + 2, −z + 2 | 2.997(1) | 165.2 |

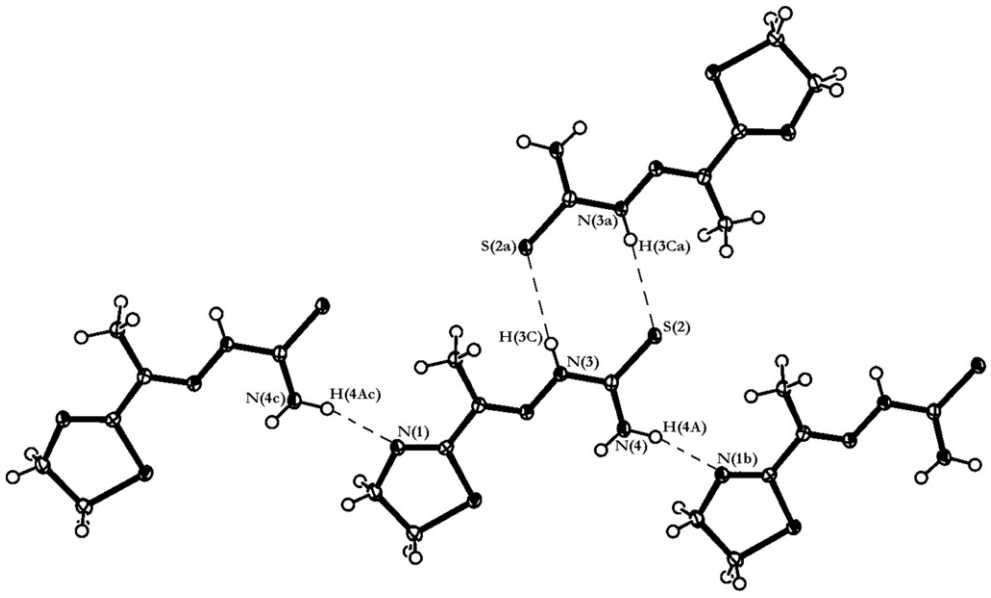


**Fig. 7.** View of the hydrogen bonds in HATtsc.

As Table 5 shows, the synthesized ligand and metal complexes **2**, **3** and **4** were found to be inactive against all the bacterial strains. The MIC values of cadmium(II) complexes **5** and **6** against *E. faecalis*, *E. coli*, *S. epidermidis* and *S. aureus*, were 50, 25, 12.5 and 25 μg/mL, respectively. Thus, in these cases, antibacterial activity increases with respect to free HATtsc ligand and cadmium(II) salts. In the case of *B. subtilis*, the activity of the complexes equals that of the salts and improves that of HATtsc. Nevertheless, **5** and **6** are inactive against *P. aeruginosa*. Finally, the antimicrobial activities in our data show that the MICs for **5** and **6** against *S. epidermidis* and *B. subtilis* are lower than for ampicilin.

It is well known that cadmium and its derivatives are more toxic for microorganisms than other trace elements at micro or millimolar levels. However, several Cd(II) complexes have been tested for their antibacterial activity with good results [30–33]. In addition, the toxicology of Cd(II) ion has been extensively studied and little cell-killing occurred at concentrations below $50 \times 10^{-3}$ to $150 \times 10^{-3}$ mM for peripheral blood cells, which indicates that this ion does not show great cytotoxic effects at sub-toxic levels [34]. In the present study, it is shown that by using *in vitro* doses of $\sim 10^{-3}$ mM of Cd(II) complex coordination to cadmium(II) improves antibacterial activity of the organic ligand, and consequently further research in this direction could find new Cd(II) compounds with potential pharmacological applications.

With regard to *B. subtilis*, the MIC values obtained for the Cd(II) salts are outstanding compared with those obtained for the other tested microorganisms in this work. It should also be noted that these low values are maintained when coordinated to HATtsc. Other Cd(II) complexes have proved to be active against *B. subtilis* [35–37] although, to the best of our knowledge, the complexes tested in this work present the lowest MIC values. One reason for this particular behaviour may be deduced from Figure included in supplementary material where a Gram tinting of *B. subtilis* can be seen. In control culture all bacilli are Gram-positive with normal size and colour. When bacteria were incubated with compound **5** (at a subinhibitory concentration of 1/2 MIC = 0.781 μg $mL^{-1}$) for 24 h, filament structures were formed. These bacteria duplicate by transverse binary fission, but apparently in this case the separation of new cells, which causes the formation of these filaments, did not take place. It is well known that many bacteria (some *Bacilli* among them) immobilize heavy metals from the broth in their cell-wall [38,39]. The effect of cadmium in *Bacillus* could be related to the inhibition of cortex-lytic enzymes involved in the degradation of the transversal wall which is formed at the moment of microbial replication [40]. This fact could explain the filament structures, since the separation of new bacteria is not completed, and could also be the reason for the activity shown by our cadmium compounds.

**Table 4**
IR spectral assignments ($cm^{-1}$) of HATtsc, **1**, **2**, **3**, **4**, **5** and **6**.

| Compound | $\nu$ (C=N)$_{endocyclic}$ | $\nu$(C=N)$_{exocyclic}$ | $\nu$(C=S) |
|---|---|---|---|
| HATtsc | 1600 | 1600 | 846 |
| 1 | 1576 | 1632 | 789 |
| | | 1607 | |
| 2 | 1576 | 1632 | 790 |
| | | 1626 | |
| 3 | 1558 | 1616 | 789 |
| 4 | 1572 | 1609 | 780 |
| 5 | 1562 | 1618 | 785 |
| 6 | 1567 | 1618 | 773 |

**Table 5**
MIC of tested complexes and inorganic salts against different microorganisms.

| Compound | MIC (μg $mL^{-1}$) | | | | | |
|---|---|---|---|---|---|---|
| | *E. faecalis* | *B. subtilis* | *S. epidermidis* | *S. aureus* | *E. coli* | *P. aeruginosa* |
| HATtsc[a] | >100 | >100 | >100 | >100 | >100 | >100 |
| **2**[b] | >100 | >100 | >100 | >100 | >100 | >100 |
| **3**[b] | >100 | >100 | >100 | >100 | >100 | >100 |
| **4**[a] | >100 | >100 | >100 | >100 | >100 | >100 |
| **5**[a] | 50 | 1.56 | 12.5 | 25 | 25 | >100 |
| **6**[a] | 50 | 3.12 | 12.5 | 25 | 25 | >100 |
| $Co(NO_3)_2$[b] | >100 | >100 | >100 | >100 | >100 | >100 |
| $Ni(NO_3)_2$[b] | >100 | >100 | >100 | >100 | >100 | >100 |
| $ZnCl_2$[a] | >100 | >100 | >100 | >100 | >100 | >100 |
| $CdCl_2$[a] | >100 | 1.56 | 50 | 100 | 100 | >100 |
| $Cd(NO_3)_2$[a] | >100 | 3.12 | 50 | 100 | >100 | >100 |
| Ampicilin | 8 | 5 | 64 | 0.25 | 8 | 8 |

[a] In DMSO.
[b] In $H_2O$.

## 5. Conclusion

The straightforward condensation of 2-acetyl-2-thiazoline and thiosemicarbazide yielding the novel Schiff base ligand has been reported. The presence of N and S donor atoms makes this an interesting compound with regard to the study of its coordination behaviour with metal ion. Spectroscopy data and X-ray single-crystal studies confirm $N_2S$ tridentate coordination of the ligand with metal ions and the antimicrobial study reveals that cadmium complexes have the best antimicrobial activity against microorganisms. The low values for MIC obtained for *B. subtilis* are due to the fact that Cd(II) compounds interfere in cell separation.

## 6. Experimental

### 6.1. General procedures

All chemicals were of reagent grade and used without any further purification. Chemical analyses of carbon, hydrogen, nitrogen and sulfur were performed by microanalytical methods using a Leco CHNS-932 microanalyser. IR spectra were recorded on a Perkin–Elmer FT-IR 1720 spectrophotometer, from KBr pellets in the 4000–370 $cm^{-1}$ range. Electronic spectra in a solution of HATtsc and complexes **1**, **2** and **3** were measured on a Shimadzu UV-3101 PC spectrophotometer using a 10 mm quartz cell. The UV–Vis–NIR reflectance spectra for **1**, **2** and **3** in the 200–2500 nm range were registered from a pellet of the sample, using a Shimadzu UV-3101 PC spectrophotometer and $BaSO_4$ as a reference. $^1H$ and $^{13}C$ NMR spectra for HATtsc and for the diamagnetic complexes were obtained with a Bruker AM 400 instrument at 400 MHz for $^1H$ NMR and 100 MHz for $^{13}C$ NMR, in DMSO-$d_6$, and also in $D_2O$ for **2**.

### 6.2. Synthesis of 2-acetyl-2-thiazoline thiosemicarbazone (HATtsc) [IUPAC name: 1-(4,5-dihydro-1,3-thiazol-2-yl)ethanone thiosemicarbazone]

A suspension of thiosemicarbazide (0.564 g, 6.2 mmol) in acetonitrile (15 mL) and 5 mL of glacial acetic acid were added to a solution of 2-acetyl-2-thiazoline (0.800 g, 6.2 mmol) in acetonitrile (5 mL). The resulting solution was heated to reflux for 2 h. Then the solution was cooled and a yellow solid appeared (0.660 g, 52%). This solid was recrystallized from acetonitrile, yielding crystals suitable for X-ray diffraction. $^1H$ NMR (400 MHz, DMSO-$d_6$, 25 °C): NH, $\delta$ = 10.79 ppm (s, 1H); $NH_2$, $\delta$ = 8.64 ppm (s, 1H), $\delta$ = 7.29 ppm (s, 1H); $CH_2$-N, $\delta$ = 4.33 ppm (t, $J$ = 8.4 Hz, 2H); $CH_2$–S, $\delta$ = 3.24 ppm (t, $J$ = 8.4 Hz, 2H); $CH_3$, $\delta$ = 2.22 (s, 3H); $^{13}C$ NMR (100 MHz, DMSO-$d_6$, 25 °C): C=S, $\delta$ = 179.6 ppm; C=$N_{thiazoline}$, $\delta$ = 168.6 ppm; C=$N_{imine}$, $\delta$ = 144.0 ppm; $CH_2$–N, $\delta$ = 65.3 ppm; $CH_2$–S, $\delta$ = 32.1 ppm; $CH_3$, $\delta$ = 13.8 ppm. *Anal.* Calc. for $C_6H_{10}N_4S_2$: C, 35.62; H, 4.98; N, 27.70; S, 31.70. Found: C, 35.61; H, 4.98; N, 27.59; S, 31.84%. IR(KBr): 3428, 3277, 3191, 3162, 3064, 1543, 1502, 1333, 1292, 1066, 947, 846, thiazoline ring vibrations: 1600, 1003, 925, 711, 698, 677, 618, 504, 446 $cm^{-1}$. UV–Vis (EtOH): $\lambda_{max}$, nm; ($\varepsilon$, L $mol^{-1}$ $cm^{-1}$) 306 (34150), 262 (10070), 240 (9260).

### 6.3. Synthesis of the complexes

#### 6.3.1. Synthesis of $[Co(ATtsc)_2]_2[CoCl_4]\cdot 2H_2O$ (**1**)

A solution containing $CoCl_2\cdot 6H_2O$ (67.5 mg, 0.1 mmol) in 1 mL ethanol:acetonitrile (2:1) was added to a solution (40 mL) of HATtsc (50.0 mg, 0.2 mmol) in ethanol:acetonitrile (2:1). The resulting solution was allowed to evaporate slowly at room temperature. After a few hours, brown prismatic crystals of considerable size were isolated from the solution. Crystals were filtered, washed with cold ether and air-dried. Yield: 65.5 mg, 92%. *Anal.* Calc. for $C_{24}H_{40}Co_3Cl_4N_{16}O_2S_8$: C, 24.85; H, 3.48; N, 19.32; S, 22.12. Found: C, 24.93; H, 3.35; N, 19.62; S, 21.95%. IR (KBr): 3462, 3403, 3328, 3180, 1625, 1607, 1531, 1313, 1293, 1061, 952, 789, thiazoline ring vibrations 1576, 1007, 743, 677, 628, 521, 446 $cm^{-1}$.

#### 6.3.2. Synthesis of $[Co(ATtsc)_2]NO_3\cdot H_2O$ (**2**)

This complex was prepared by reacting an ethanol:acetonitrile (2:1) solution (1 mL) of $Co(NO_3)_2\cdot 6H_2O$ (71.9 mg, 0.1 mmol) with a solution (40 mL) of HATtsc (50.0 mg, 0.2 mmol) in the same solvent. Brown crystals were isolated after a slow evaporation of the solution at room temperature. The crystals were filtrated, washed with cold ether and finally air-dried. Yield: 55.3 mg, 88%. $^1H$ NMR (400 MHz, DMSO-$d_6$, 25 °C): $NH_2$, $\delta$ = 8.38 ppm (s, 2H), $CH_2$–N, $\delta$ = 3.82 ppm (t, $J$ = 8.4 Hz, 2H); $CH_2$–S, $\delta$ = 3.72 ppm (t, $J$ = 10.4 Hz, 2H); $CH_3$, $\delta$ = 2.45 (s, 3H); $^{13}C$ NMR (100 MHz, DMSO-$d_6$, 25 °C): C=S, $\delta$ = 183.3 ppm; C=$N_{thiazoline}$, $\delta$ = 175.4 ppm; C=$N_{imine}$, $\delta$ = 147.4 ppm; $CH_2$–N, $\delta$ = 56.2 ppm; $CH_2$=S, $\delta$ = 32.7 ppm; $CH_3$, $\delta$ = 17.1 ppm. *Anal.* Calc. for $C_{12}H_{20}CoN_9O_4S_4$: C, 26.72; H, 3.74; N, 23.37; S, 23.77. Found: C, 26.57; H, 3.61; N, 23.08; S, 23.58%. IR (KBr): 3413, 3300, 3151, 1633, 1626, 1533, 1385, 1316, 1298, 1061, 952, 790, thiazoline ring vibrations 1576, 990, 736, 692, 678, 618, 532, 442 $cm^{-1}$.

#### 6.3.3. Synthesis of $[Ni(HATtsc)_2](NO_3)_2$ (**3**)

$Ni(NO_3)_2\cdot 6H_2O$ (71.6 mg, 0.1 mmol) dissolved in ethanol:acetonitrile (2:1) (1 mL) was added to a ethanol:acetonitrile (2:1) solution (40 mL) of HATtsc (50.0 mg, 0.2 mmol). The resulting solution was allowed to evaporate slowly at room temperature. After a few days, red-brown prismatic crystals of considerable size were isolated from the solution. Crystals were separated by filtration, washed with cold ether and air-dried. Yield: 70.2 mg, 91%. *Anal.* Calc. for $C_{12}H_{20}N_{10}NiO_6S_4$: C, 24.54; H, 3.43; N, 23.84; S, 21.83. Found: C, 24.35; H, 3.27; N, 23.46; S, 21.60%. IR (KBr): 3387, 3292, 3150, 1616, 1385, 1322, 1284, 1076, 1007, 948, 789, thiazoline ring vibrations 1558, 1007, 698, 683, 602, 508, 458 $cm^{-1}$.

#### 6.3.4. Synthesis of $[ZnCl_2(HATtsc)]\cdot CH_3CN$ (**4**)

This complex was isolated from an ethanol:acetonitrile (2:1) solution (1 mL) of $ZnCl_2$ (33.6 mg, 0.2 mmol) that was added to an ethanol:acetonitrile (2:1) solution (40 mL) of HATtsc (50.0 mg, 0.2 mmol). After several days, yellow prismatic crystals of considerable size were isolated from the solution at room temperature. Crystals were separated by filtration, washed with cold ether and air-dried. Yield: 60.6 mg, 65%. $^1H$ NMR (400 MHz, DMSO-$d_6$, 25 °C): NH, $\delta$ = 10.82 ppm (s, 1H); $NH_2$, $\delta$ = 8.67 ppm (s, 1H), $\delta$ = 7.31 ppm (s, 1H); $CH_2$–N, $\delta$ = 4.34 ppm (t, $J$ = 7.8 Hz, 2H); $CH_2$–S, $\delta$ = 3.26 ppm (t, $J$ = 7.4 Hz, 2H); $CH_3$, $\delta$ = 2.22 (s, 3H). *Anal.* Calc. for $C_8H_{13}Cl_2N_5S_2Zn$: C, 25.31; H, 3.45; N, 18.45; S, 16.89. Found: C, 24.98; H, 3.31; N, 18.49; S, 16.52%. IR (KBr): 3446, 3367, 3277, 3189, 2089, 1609, 1317, 1277, 1073, 943, 780, thiazoline ring vibrations 1572, 1003, 697, 682, 618, 505, 452 $cm^{-1}$.

#### 6.3.5. Synthesis of $[\{CdCl(HATtsc)\}_2(\mu\text{-}Cl)_2]\cdot 2H_2O$ (**5**)

An ethanol:acetonitrile (2:1) solution (1 mL) containing $CdCl_2\cdot 2.5H_2O$ (56.2 mg, 0.2 mmol) was added to 40 mL of a solution of HATtsc (50.0 mg, 0.2 mmol) in the same solvent. The resulting solution was allowed to evaporate slowly at room temperature. After a few hours, colourless prismatic crystals of considerable size were isolated from the solution. Crystals were filtered, washed with cold ether and air-dried. Yield: 81.0 mg, 81%. $^1H$ NMR (400 MHz, DMSO-$d_6$, 25 °C): NH, $\delta$ = 10.83 ppm (s, 1H); $NH_2$, $\delta$ = 8.68 ppm (s, 1H), $\delta$ = 7.33 ppm (s, 1H); $CH_2$–N, $\delta$ = 4.34 ppm (t, $J$ = 8.4 Hz, 2H); $CH_2$–S, $\delta$ = 3.27 ppm (t, $J$ = 8.4 Hz, 2H); $CH_3$, $\delta$ = 2.23 (s, 3H). *Anal.* Calc. for $C_{12}H_{24}Cd_2Cl_4N_8O_2S_4$: C, 17.84; H, 2.99; N, 13.88; S, 15.88.

Found: C, 17.83; H, 2.56; N, 14.00; S, 15.93%. IR (KBr): 3448, 3397, 3296, 3171, 3067, 1618, 1507, 1317, 1273, 1068, 941, 785, thiazoline ring vibrations 1562, 981, 697, 685, 622, 557, 455 $cm^{-1}$.

#### 6.3.6. Synthesis of [{Cd($NO_3$)(HATtsc)}$_2$($\mu$-$NO_3$)$_2$] (**6**)

This complex was isolated from an ethanol:acetonitrile (2:1) solution (1 mL) of $Cd(NO_3)_2 \cdot 4H_2O$ (75.9 mg, 0.2 mmol) that was added to an ethanol:acetonitrile (2:1) solution (40 mL) of HATtsc (50.0 mg, 0.2 mmol). After several days, yellow prismatic crystals of considerable size were isolated from the solution at room temperature. Crystals were separated by filtration, washed with cold ether and air-dried. Yield: 84.6 mg, 83%. $^1$H NMR (400 MHz, DMSO-$d_6$, 25 °C): NH, $\delta = 10.85$ ppm (s, 1H); $NH_2$, $\delta = 8.68$ ppm (s, 1H), $\delta = 7.39$ ppm (s, 1H); $CH_2$–N, $\delta = 4.32$ ppm (t, $J = 8.2$ Hz, 2H); $CH_2$–S, $\delta = 3.28$ ppm (t, $J = 8.4$ Hz, 2H); $CH_3$, $\delta = 2.22$ (s, 3H). *Anal.* Calc. for $C_{12}H_{20}Cd_2N_{12}O_{12}S_4$: C, 16.42; H, 2.30; N, 19.15; S, 14.60. Found: C, 16.55; H, 2.14; N, 19.10; S, 14.88%. IR (KBr): 3390, 3281, 3187, 3058, 1618, 1461, 1384, 1324, 1309, 1270, 1071, 1030, 943, 835, 773, thiazoline ring vibrations 1567, 980, 734, 708, 697, 727, 697, 682, 627, 552, 458 $cm^{-1}$.

### 6.4. Crystal structure determination

X-ray diffraction measurements were performed using a Bruker SMART CCD diffractometer with Mo K$\alpha$ radiation ($\lambda = 0.71073$ Å, graphite monochromator). The first fifty frames were measured at the end of the data collection to monitor instrument and crystal stability. Absorption corrections were applied using the program SADABS [41]. The structures were solved by direct methods and subsequent Fourier differences using the SHELXS-97 [42] program and refined by full-matrix least-squares on $F^2$ with SHELXL-97 [42], included in WINGX [43] package. All non-hydrogen atoms were refined with anisotropic displacement parameters, except for oxygen atoms of water molecules in compound **2** which were refined assuming isotropic displacement parameters. All hydrogen atoms attached to carbon and nitrogen atoms were positioned geometrically, with $U_{iso}$ values derived from $U_{eq}$ values of the corresponding carbon and nitrogen atoms. However, hydrogen atoms of the water molecules were detected by Fourier differences and were refined with fixed O–H and H–H distances (0.957(3) and 1.513(3) Å, respectively), except for **1** in which they were ignored because of the impossibility of obtaining a correct model. In complex **2** one of the two nitrate ions present in the molecule was successfully modellized while the other was not. As a result, the final electron density map contained various electron density peaks clustered in one region of the unit cell. However, this problem was solved by using the SQUEEZE routine in PLATON [44], since the peaks represented a disordered nitrate ion. The unit cell contains four cavities centered at (1/4, 3/4, 0), (3/4, 1/4, 0), (1/4, 1/4, 1/2) and (3/4, 3/4, 1/2), which posses electronic density. The volume of each cavity is 113.5 Å$^3$, with a total of approximately 34 electrons in each cavity, corresponding approximately to the 32 calculated electrons for a nitrate ion in each cavity. Graphical representations of the molecular structures were generated using ORTEP3 [45]. Experimental details of the crystal structure determinations are listed in Tables 6 and 7.

**Table 6**
Crystal data and structure refinement for HATtsc and compounds **1**–**4**.

| | HATtsc | **1** | **2** | **3** | **4** |
|---|---|---|---|---|---|
| Crystal shape | Prism | Prism | Prism | Prism | Prism |
| Colour | Yellow | Brown | Brown | Red-brown | Yellow |
| Size (mm) | 0.48 × 0.27 × 0.26 | 0.46 × 0.19 × 0.15 | 0.44 × 0.37 × 0.24 | 0.34 × 0.30 × 0.10 | 0.27 × 0.2 × 0.16 |
| Chemical formula | $C_6H_{10}N_4S_2$ | $C_{24}H_{36}Cl_4Co_3N_{16}O_2S_8$ | $C_{12}H_{20}CoN_9O_4S_4$ | $C_{12}H_{20}N_{10}NiO_6S_4$ | $C_8H_{13}Cl_2N_5S_2Zn$ |
| Formula weight | 202.3 | 1155.76 | 1083.08 | 587.33 | 379.62 |
| Crystal system | Monoclinic | Monoclinic | Monoclinic | Monoclinic | Triclinic |
| Space group | C 2/c | C 2/c | C 2/c | P $2_1$/c | P −1 |
| Unit cell dimensions | | | | | |
| *a* (Å) | 16.044(1) | 24.920(2) | 37.034(6) | 13.97(1) | 7.526(2) |
| *b* (Å) | 8.683(1) | 12.094(1) | 14.181(2) | 8.444(7) | 9.075(2) |
| *c* (Å) | 13.881(1) | 15.756(1) | 8.693(1) | 21.96(2) | 12.108(3) |
| α (°) | | | | | 72.383(3) |
| β (°) | 110.928(1) | 113.862(1) | 102.656(3) | 108.40(1) | 74.221(4) |
| γ (°) | | | | | 82.144(4) |
| Cell volume (Å$^3$) | 1806.1(2) | 4342.5(4) | 4454.6(12) | 2459(3) | 757.1(3) |
| Z | 8 | 4 | 4 | 4 | 2 |
| *T* (K) | 298 | 298 | 293 | 293 | 293 |
| $D_{calc}$ (g cm$^{-3}$) | 1.488 | 1.768 | 1.522 | 1.587 | 1.665 |
| μ (mm$^{-1}$) | 0.539 | 1.812 | 1.174 | 1.178 | 2.239 |
| F(000) | 848 | 2340 | 2100 | 1208 | 384 |
| $\theta$ range | 2.7–28.3 | 1.8–28.3 | 1.1–27.1 | 2.1–27.1 | 1.8–26.4 |
| Index ranges | $-20 \le h \le 21$, $-9 \le k \le 11$, $-18 \le l \le 17$ | $-32 \le h \le 22$, $-15 \le k \le 15$, $-13 \le l \le 21$ | $-47 \le h \le 46$, $0 \le k \le 18$, $0 \le l \le 11$ | $-17 \le h \le 16$, $0 \le k \le 10$, $0 \le l \le 28$ | $-8 \le h \le 9$, $-10 \le k \le 11$, $0 \le l \le 15$ |
| Independent reflections | 2045 | 4981 | 4901 | 5402 | 3085 |
| Observed reflections [F > 4.0σ(F)] | 1943 | 4426 | 3600 | 3952 | 2410 |
| Data completeness | 0.99 | 0.988 | 0.996 | 0.999 | 0.995 |
| Max/min transmission | 0.782/0.872 | 0.763/0.667 | 0.766/0.626 | 0.891/0.690 | 0.696/0.588 |
| No. of ref. parameters | 149 | 260 | 257 | 300 | 165 |
| *R* [F > 4.0σ(F)][a] | 0.027 | 0.033 | 0.052 | 0.041 | 0.033 |
| *wR* [F > 4.0σ(F)][b] | 0.072 | 0.087 | 0.162 | 0.110 | 0.083 |
| GOF[c] | 1.077 | 1.06 | 1.109 | 0.969 | 1.053 |
| $\rho_{max}$, $\rho_{min}$ (e Å$^{-3}$) | 0.328/−0.312 | 0.804/−0.544 | 1.08/−0.794 | 0.618/−0.454 | 0.38/−0.385 |

[a] $R = \Sigma||F_o| - |F_c||/\Sigma|F_o|$
[b] $R = \{\Sigma[w(F_o^2 - F_c^2)^2]/\Sigma[w(F_o^2)^2]\}^{1/2}$
[c] The goodness-of-fit (GOF) equals $\{\Sigma[w(F_o^2 - F_c^2)^2]/(N_{rflns} - N_{params})\}^{1/2}$

**Table 7**
Crystal data and structure refinement for compounds **5** and **6**.

| | **5** | **6** |
|---|---|---|
| Crystal shape | Prism | Prism |
| Colour | Colourless | Yellow |
| Size (mm) | 0.18 × 0.1 × 0.08 | 0.43 × 0.33 × 0.16 |
| Chemical formula | $C_{12}H_{24}Cd_2Cl_4N_8O_2S_4$ | $C_{12}H_{20}Cd_2N_{12}O_{12}S_4$ |
| Formula weight | 807.23 | 877.50 |
| Crystal system | Triclinic | Monoclinic |
| Space group | P −1 | P $2_1$/n |
| Unit cell dimensions | | |
| *a* (Å) | 8.182(2) | 8.836(1) |
| *b* (Å) | 8.832(2) | 14.109(1) |
| *c* (Å) | 10.457(2) | 11.004(1) |
| α (°) | 76.890(3) | |
| β (°) | 72.755(3) | 94.015(1) |
| γ (°) | 65.092(3) | |
| Cell volume (Å$^3$) | 650.0(2) | 16.044(1) |
| Z | 1 | 2 |
| *T* (K) | 120 | 100 |
| $D_{calc}$ (g cm$^{-3}$) | 2.062 | 2.129 |
| μ (mm$^{-1}$) | 2.396 | 1.938 |
| F(000) | 396 | 864 |
| θ range | 2.0–26.7 | 2.3–28.3 |
| Index ranges | $-9 \le h \le 10$, $-10 \le k \le 11$, $0 \le l \le 13$ | $-11 \le h \le 11$, $-11 \le k \le 18$, $-13 \le l \le 13$ |
| Independent reflections | 2745 | 3120 |
| Observed reflections [F > 4.0σ(F)] | 2210 | 3003 |
| Data completeness | 0.994 | 0.994 |
| Max/min transmission | 0.831/0.672 | 0.733/0.474 |
| No. of ref. parameters | 161 | 191 |
| *R* [F > 4.0σ(F)][a] | 0.030 | 0.022 |
| *wR* [F > 4.0σ(F)][b] | 0.060 | 0.052 |
| GOF[c] | 1.033 | 1.162 |
| $\rho_{max}$, $\rho_{min}$ (e Å$^{-3}$) | 0.552/−0.619 | 0.401/−0.492 |

[a] $R = \Sigma||F_o| - |F_c||/\Sigma|F_o|$
[b] $R = \{\Sigma[w(F_o^2 - F_c^2)^2]/\Sigma[w(F_o^2)^2]\}^{1/2}$
[c] The goodness-of-fit (GOF) equals $\{\Sigma[w(F_o^2 - F_c^2)^2]/(N_{rfIns} - N_{params})\}^{1/2}$

### 6.5. Antibacterial activity

Antibacterial activities were screened *in vitro* against the following organisms, obtained directly from ATCC collections: *Staphylococcus epidermidis* ATCC 12228, *Staphylococcus aureus* ATCC 29213, *Enterococcus faecalis* ATCC 29212, *Bacillus subtilis* ATCC 12432, *Escherichia coli* ATCC 25922 and *Pseudomonas aeruginosa* ATCC 27853. All microorganisms were stored at −80 °C in porous beads (Microbank, Pro-Lab Diagnostics, Austin, USA). The tested substances were dissolved in distilled water or DMSO at a concentration of 2 mg mL$^{-1}$, except for inorganic salts solved in DMSO for which the initial concentration was 1 mg mL$^{-1}$. Stock solutions were prepared and dilutions were made according to protocols of the Antibacterial Susceptibility Test for Bacteria by a broth dilution method using Mueller–Hinton medium according to the guidelines of the Clinical and Laboratory Standards Institute, CLSI (formerly NCCLS) [28]. All strains were incubated at 37 °C for 24 h to obtain cultures, and then transferred to Mueller–Hinton Broth medium (Oxoid Ltd., Basingstoke, Hants., England). The microorganisms were diluted in fresh trypticase soy broth (TSB) to a turbidity equivalent to a 0.5 McFarland standard and then diluted 1/100 to obtain an inoculum of approximately $10^6$ cfu/mL. The minimum inhibitory concentration (MIC) determination of compounds was evaluated by the quantitative polystyrene microtiter plate method, using broth microdilution [28]. All strains were incubated for 24 h at 37 °C with different concentrations of compounds in Mueller–Hinton. For quantitative measurements, wells of sterile 96-well polystyrene flat-bottomed microtiter plates (Greiner bio-one, Nurburg, Germany) were each filled with 100 μL of different concentrations of compounds in Mueller–Hinton and 100 μL of each cell suspension (~$10^6$ cfu/mL), in duplicate. Negative control wells contained only compounds and strain growth was used as a positive control. The MIC determination of compounds was determined by reading each well at 492 nm in an automated microplate reader (Model Anthos 2020, Anthos Labtec Instruments, Austria), and was defined as the lowest concentration of compounds which inhibited visible growth at 37 °C after overnight incubation. Each assay was performed in duplicate and repeated three or more times.

## Acknowledgements

The authors would like to thank the Junta de Extremadura (III PRI+D+I) and the FEDER (Project PRI08A022). P. Torres-García thanks the Universidad de Extremadura for his Ph.D. fellowship.

## Appendix. Supplementary data

CCDC 759079 to 759085 contain the supplementary crystallographic data for this paper. These data can be obtained free of charge via http:\\www.ccdc.cam.ac.uk/conts/retrieving.html, or from the Cambridge Crystallographic Data Centre, 12 Union Road, Cambridge CB2 1EZ, UK; fax: (+44) 1223-336-033; e-mail: deposit@ccdc.cam.ac.uk.

## Appendix. Supplementary data

Supplementary data related to this article can be found online at doi:10.1016/j.ejmech.2010.10.030.

## References

[1] A. Ino, A. Murabayashi, Tetrahedron 55 (1999) 10271–10282.
[2] L.C. Craig, W.F. Phillips, M. Burachik, Biochem 8 (1969) 2348–2356.
[3] T.S. Lobana, R. Sharma, G. Bawa, S. Khanna, Coord. Chem. Rev. 253 (2009) 977–1055.
[4] P. Genova, T. Varadinova, A.I. Matesanz, D. Marinova, P. Souza, Toxicol. Appl. Pharmacol. 197 (2004) 107–112.
[5] M.C. Rodríguez-Argüelles, E.C. López-Silva, J. Sanmartín, A. Bacchi, C. Pelizzi, F. Zani, Inorg. Chim. Acta 357 (2004) 2543–2552.
[6] A. Cukurovali, I. Yilmaz, S. Gur, C. Kazaz, Eur. J. Med. Chem. 41 (2006) 201–207.
[7] W.X. Hu, W. Zhou, C. Xia, X. Wen, Bioorg. Med. Chem. Lett. 16 (2006) 2213–2218.
[8] K. Alomar, A. Landreau, M. Kempf, M.A. Khan, M. Allain, G. Bouet, J. Inorg. Biochem. 104 (2010) 397–404.
[9] S. Chandra, S. Raizada, M. Tyagi, P.K. Sharma, Spectrochim. Acta A 69 (2008) 816–821.
[10] N.C. Kasuga, K. Sekino, M. Ishikawa, A. Honda, M. Yokoyama, S. Nakano, N. Shimada, C. Koumo, K. Nomiya, J. Inorg. Biochem. 96 (2003) 298–310.
[11] T. Doornbos, H.G. Peer, Recl. Trav. Chim. Pays-Bas 91 (1972) 711–728.
[12] J.S. Casas, E.E. Castellano, J. Ellena, M.S. García-Tasende, A. Sánchez, J. Sordo, A. Touceda, Polyhedron 28 (2009) 1029–1039.
[13] M. Joseph, V. Suni, C.R. Nayar, M.R.P. Kurup, H.K. Fun, J. Mol. Struct. 705 (2004) 63–70.
[14] E. Labisbal, K.D. Haslow, A. Sousa-Pedrares, J. Valdés-Martínez, S. Hernández-Ortega, D.X. West, Polyhedron 22 (2003) 2831–2837.
[15] A.W. Addison, T.N. Rao, J. Reedijk, J. Van Rijn, G.C. Veschoor, J. Chem. Soc. Dalton Trans. (1984) 1349–1356.
[16] E.L. Muetterties, J. Guggemberger, J. Am. Chem. Soc. 96 (1974) 1748–1756.
[17] Y. Tian, C. Duan, C. Zhao, X. You, Inorg. Chem. 36 (1997) 1247–1252.
[18] K.A. Ketcham, I. García, J.K. Swearingen, A.K. El-Sawaf, E. Bermejo, A. Castiñeiras, D.X. West, Polyhedron 21 (2002) 859–865.
[19] J.M. Pérez, A.I. Matesanz, A. Martín-Ambite, P. Navarro, C. Alonso, P. Souza, J. Inorg. Biochem. 75 (1999) 255–261.
[20] D.K. Sau, R.J. Butcher, S. Chaudhuri, N. Saha, Polyhedron 23 (2004) 5–14.
[21] D. Kovala-Demertzi, P.N. Yadav, J. Wiecek, S. Skoulika, T. Varadinova, M.A. Demertzis, J. Inorg. Biochem. 100 (2006) 1558–1567.
[22] A.B.P. Lever, Inorganic Electronic Spectroscopy. Elsevier, Amsterdan, 1984.
[23] P.F. Rapheal, E. Manoj, M.R. Prathapachandra Kurup, E. Suresh, Polyhedron 26 (2007) 607–616.
[24] S. Iwatsuki, H. Kato, K. Obeyama, S. Funahashi, N. Koshino, K. Kashiwabara, T. Suzuki, H.D. Takagi, Inorg. Chem. Commun. 3 (2000) 501–504.
[25] C.A. Sharrad, L.R. Gahan, Polyhedron 23 (2004) 2217–2226.

[26] E. Viñuelas-Zahínos, F. Luna-Giles, P. Torres-García, A. Bernalte-García, Polyhedron 28 (2009) 1362–1368.
[27] L. Sacconi, F. Mani, A. Bencini, in: G. Wilkinson (Ed.), Comprehensive Coordination Chemistry, Late Transitions Elements, vol. 5, Pergamon Press, Oxford, 1987, p. 51.
[28] National Committee for Clinical Laboratory Standards, Methods for Dilution Antibacterial Susceptibility Test for Bacteria that Grow Aerobically Approved Standard M7–A6, sixth ed. NCCLS, Wayne, Pennsylvania, 2003.
[29] S. Erazo, R. Negrete, M. Zaldivar, N. Backhouse, C. Delporte, I. Silva, E. Belmonte, J.L. López-Pérez, A. San Feliciano, Planta Med. 68 (2002) 66–67.
[30] D.U. Miodragović, D.M. Mitić, Z.M. Miodragović, G.A. Bogdanović, Z.J. Vitnik, M.D. Vitirović, M.D. Radulović, B.J. Nastasijević, I.O. Juranić, K.K. Anđelković, Inorg. Chim. Acta 361 (2008) 86–94.
[31] N.A. Pulina, P.A. Mokin, V.V. Zalesov, T.F. Odegova, M.V. Tomilov, K.V. Yatsenko, Pharm. Chem. J. 42 (2008) 389–391.
[32] N.H. Patel, H.M. Parekh, M.N. Patel, Pharm. Chem. J. 41 (2007) 78–81.
[33] M. Sönmez, I. Berber, E. Akbaş, Eur. J. Med. Chem. 41 (2006) 101–105.
[34] M.D. Enger, C.E. Hildebrand, C.C. Stewart, Toxicol. Appl. Pharm. 69 (1983) 214–224.
[35] N. Raman, J.D. Raja, A. Sakthivel, Russ. J. Coord. Chem. 34 (2008) 400–406.
[36] A. Uğur, B. Mercimek, M. Ali Özler, N. Şahin, Transit. Met. Chem. 25 (2000) 421–425.
[37] M.T.H. Tarafder, K. Teng Jin, F.A. Crouse, A.M. Ali, B.M. Yamin, H.-K. Fun, Polyhedron 21 (2002) 2547–2554.
[38] M.D. Mullen, D.C. Wolf, F.G. Ferris, T.J. Beveridge, C.A. Flemming, G.W. Bailey, Appl. Environ. Microbiol. 55 (1989) 3143–3149.
[39] J.J. Doyle, R.T. Marshall, W.H. Pfander, Appl. Microbiol. 29 (1975) 562–564.
[40] Y. Nakatani, M. Imagawa, T. Nishihara, M. Kondo, Microbiol. Immunol. 29 (1985) 119–126.
[41] Bruker AXS Inc, SADABS, Version 2.03. Bruker AXS Inc., Madison, WI, 2001.
[42] G.M. Sheldrick, Acta Crystallogr. A 64 (2008) 112–122.
[43] L.J. Farrugia, J. Appl. Crystallogr. 32 (1999) 837–838.
[44] A.L. Spek, J. Appl. Crystallogr. 36 (2003) 7–13.
[45] L.J. Farrugia, J. Appl. Crystallogr. 30 (1997) 565.